

# Power Sharing Strategy for Photovoltaic based Distributed Generators Operating in Parallel

Urvi N. Patel and Hiren H. Patel

**Abstract**— In many countries, the grid-code or standards do not allow the Photovoltaic (PV) inverters to exchange reactive power with the grid. Recently, some countries have relaxed the standards. Hence, capacity of the inverters to control reactive power must be utilized. However, the reactive power that a PV inverter can supply is constrained by the maximum power that a PV array generates and changes with the environmental conditions. A reactive power sharing algorithm is proposed that not only ensures proper distribution of reactive power amongst the inverters, but also ensures that the maximum power generated by PV is supplied to the grid. In case of identical PV inverters, the algorithm operates all inverters at nearly equal apparent power leading to nearly equal percentage utilization of the inverters, thereby achieving uniform heating of the similar devices of the inverters. The algorithms are further investigated for power sharing amongst PV inverters of unequal ratings. It is highlighted that the proposed algorithm results into the least change in the utilization factor of a PV inverter, whose power changes due to the change in environmental conditions. The effectiveness of the algorithm over other algorithms in sharing power amongst inverters is displayed through MATLAB/Simulink simulations.

**Keywords** — Photovoltaic, Reactive power, Power sharing.

## I. INTRODUCTION

Last couple of decades have experienced significant rise in the electricity generation from non-conventional energy sources like wind and solar. It is attributed mainly by the increased environmental concern, fast depletion of conventional energy sources, increase in cost of conventional energy sources, and decrease in the cost of renewable based energy generation. In recent years, one of the renewable sources that has seen the fastest growth and penetration in the electrical grid is the solar photovoltaic (PV). The reason for the increase in penetration is the reduced cost of PV system and the encouraging feed-in-tariff policies by the governments. However, increased penetration of PV sources has also given rise to several challenges.

The challenges are mainly due to the dependence of PV source's performance on the environment, which makes it intermittent and uncertain in nature. PV source is connected to the grid through the static power converters [1]. Thus, it is inertia-less source of energy unlike the conventional rotational generators. Hence, if the energy generation in the grid is highly dominated by inertia-less PV (i.e. in a weak grid), the sudden change in output power of PV resulting from the sudden change in irradiation, may affect the stability of grid and the systems connected with the utility. Also, if the power electronic

converters are not controlled appropriately in such weak electrical grid or a microgrid (MG), they are likely to create issues like harmonic injection, change in voltage levels and power flow, flicker, resonance, mal-operation of protection scheme etc.

On the contrary, if the power electronic converters are properly controlled [2]-[3], they can improve the voltage profile and performance of the MG. This can be achieved if PV systems, which are usually commissioned to supply active power, are allowed to inject desired reactive power into the grid. PV systems are usually designed with reasonable margins, and most of the times operate under lightly loaded conditions (in fact inactive at night time). Thus, there is a room for reactive power injection to keep the voltage at a desirable level. This objective, along with the transfer of maximum power generated by PV, can be achieved by controlling the amplitude and phase angle of the output voltage of the inverter. The task becomes challenging when several such PV based distributed energy generators are operating in a MG, which even comprises of other types of renewable energy sources.

PV inverters are commonly controlled as current controlled source using  $P-Q$  control strategy to exchange active and reactive  $P$  and  $Q$  respectively, with the microgrid [4]. In islanding mode i.e. when main grid is disconnected, the voltage  $V$  and frequency  $\omega$  are controlled, using  $P-\omega$  and  $Q-V$  droop control methods to share active and reactive power amongst the distributed generators (DG) [5]-[7]. Battery storage is essential in such system when islanded, in order to maintain power balance in the system.

Lasseter *et al.*, have presented flexible control and proper coordination amongst DG sources to overcome some problems associated with PV and other non-conventional sources operating simultaneously in a MG [3]. Local power management system for coordination of various DG sources to manage active and reactive power successfully is addressed in [8]-[10]. In [8], fundamental algorithm employing hierarchical droop control of power management is presented, where inverter control is considered as primary control whereas Microgrid Central Controller (MGCC) is under secondary control. Secondary control focuses on power management and optimization algorithm to optimize performance of MG.

Power management system plays very important role when MG is having many PV connected inverters, as rapidly varying irradiation condition may cause voltage sags and swells that result in degradation of power quality [16]-[20]. To regulate voltage under such transient condition, PV inverters must have

U. N. Patel is with Department of Electrical Engineering, C. K. Pithawala College of Engineering and Technology, Surat, India. (email: urvi.patel@ckpceet.ac.in).

H. H. Patel is with the Department of Electrical Engineering, Sarvajani College of Engineering & Technology, Surat, India. (e-mail: hiren.patel@scet.ac.in).

the capability to match-up the VAR requirement quickly [11]. As active power delivered by inverter depends on maximum power that PV can generate under given (environmental) conditions, it is necessary to allocate reactive power amongst inverters in a proper way to have uniform loading of the inverters and to also avoid over loading of inverters [12]. An accurate reactive power sharing control that shares reactive power equally amongst inverters is presented [13]. Total reactive power of the system is calculated by MGCC and the information is passed to all inverters through communication link. Though this method shares reactive power accurately amongst the inverters, in case when active power varies with the change in irradiation, it fails to accurately share the reactive power amongst the PV inverters. It may also cause inverter to work beyond its nominal apparent power transfer capability.

In [14], reactive power algorithm is presented which takes into account apparent power limit of each PV connected inverter as well as active power delivered by each PV inverter. Optimal reactive power strategy [15] assigns reactive power to each inverter such that entire system can achieve maximum reactive power transfer capability. However, these algorithms are unable to uniformly utilize apparent power capability of each inverter.

The paper proposes an approach to overcome these drawbacks. The proposed reactive power algorithm first determines the active power that PV inverters are supplying under given conditions and based on the available margin it assigns the reactive powers to the inverters. Section II introduces system configuration and control scheme employed for operating PV inverters while the secondary control algorithm implemented in MGCC for accurate reactive power sharing is presented in section III. The results of the simulation study performed in MATLAB/Simulink are included in section IV to demonstrate the performance of algorithm for PV inverters operating in parallel for two different cases: (i) all inverters with equal ratings and (ii) inverters with unequal ratings.

## II. SYSTEM DESCRIPTION AND CONTROL

Fig.1 shows the system configuration considered for evaluation of the proposed algorithm. The microgrid comprises of four identical distributed energy generators that along with the main grid (or a relatively stiff source) supply the local loads. Each DG unit consists of PV as a primary energy source, a three phase inverter and an LC filter. The inverters not only extract the maximum power from the PV but also supply sinusoidal current to the load and grid.  $PV_i$  shown in Fig. 1 represents a PV array with its dc-dc converter operated with maximum power point tracking control. The DGs are connected to the PCC through a transformer, which for the sake of simplicity, is not shown in Fig.1.

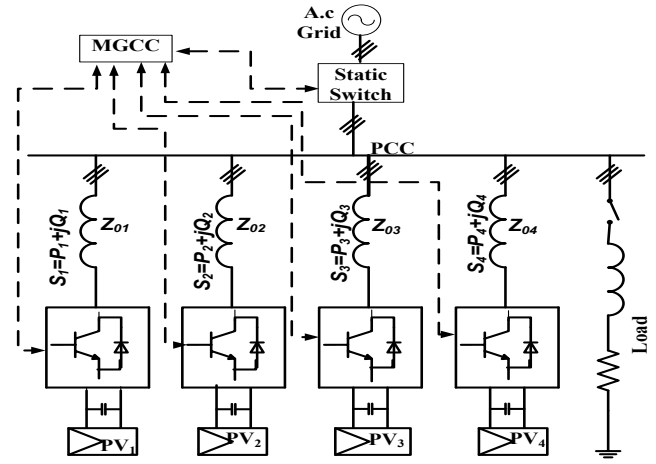


Fig.1. System configuration of a Microgrid having four DGs

The impedances  $Z_{oi}$ , where 'i' represents  $i^{th}$  DG, takes into account the impedance of interfacing inductor, the impedance of cable and isolation transformer. Active and reactive power management task is performed by MGCC unit using low bandwidth communication links.

Microgrid hierarchical structure consists of mainly primary, secondary and tertiary control [10], [11]. Primary control covers inverters' control present in microgrid whereas secondary control consists of MGCC unit. Tertiary control provides interaction between multiple microgrid and utility grid. Primary and secondary controls are used in this paper while tertiary control is not required at this stage.

Inverter control is achieved by active-reactive power ( $P-Q$ ) control method [4].  $P-Q$  method is used to operate inverter as a controlled current source for desired active and reactive power transfer with grid. Inverter output current is tightly regulated by inner current control loop. Reference currents for current control loop are provided by outer power control loop according to power references provided by MGCC. Phase locked loop (PLL) used for grid synchronization provides desired angle ( $\rho$ ) for  $abc$  to  $dq$  frame transformation. Fig.2 shows control circuit diagram for one of the inverters.

Fig.3 shows the details of the power and current control loops shown in Fig. 2. The voltage  $V_{dc}$ , across capacitor C is maintained at a desired voltage,  $V_{dcref}$  by a voltage control loop.

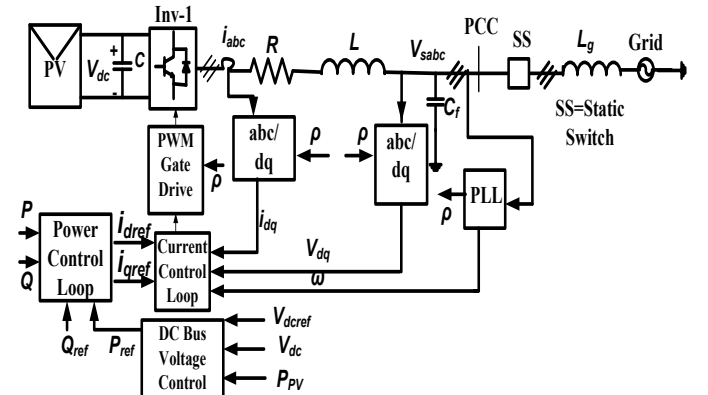


Fig. 2. Control scheme of PV inverter

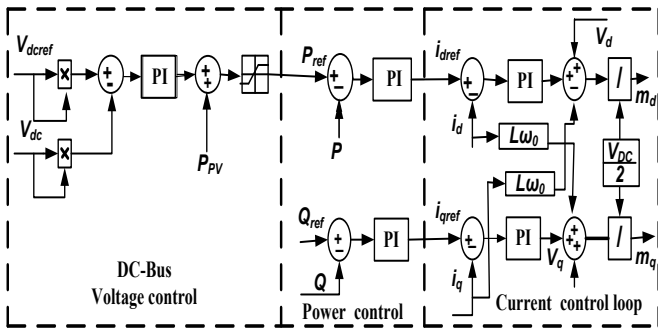


Fig.3. Active-reactive power control

To maintain this voltage constant it is ensured that the power obtained from PV array,  $P_{pv}$  is entirely transferred to the grid side. This is done through the power control loop, which compares actual DG output power ( $P$ ) with reference power ( $P_{ref}$ ). The reactive power reference ( $Q_{ref}$ ) is obtained using the algorithm presented in the next section.  $P_{ref}$  and  $Q_{ref}$  are used to generate required current references  $i_{dref}$  and  $i_{qref}$  for the current control loop. The direct and quadrature axes components of the inverter output currents  $i_d$  and  $i_q$ , respectively, are obtained through  $d$ - $q$  transformation. The current control loop finally determines the direct and quadrature axes modulation indices,  $m_d$  and  $m_q$ , respectively.

### III. PROPOSED REACTIVE POWER SHARING ALGORITHM

As the active power that PV inverters supply is directly dependent on the environmental conditions (mainly irradiation), most of the times the inverters do not operate at their rating and hence, their capacity is not utilized fully. The available margin varies with the irradiation, with maximum at night or when irradiation is the least. The reactive power sharing algorithm shown in Fig. 4 relies on assigning the reactive power amongst the inverters based on the margin available with each of them.

The algorithm starts with initializing the number of inverters ( $m$ ) and the apparent ratings of the inverters ( $S_{iN}$ ), where ' $i$ ' stands for  $i^{\text{th}}$  inverter. The output power of the PV systems ( $P_i$ ) is obtained from the maximum power point tracker (MPPT), which ensures that the PV system operates at its maximum (active) power point.

As the apparent power ratings ( $S_{iN}$ ) of the inverters are known and as the inverter must be operated to deliver active power ( $P_i$ ) to the grid side, the available reactive power ( $Q_i$ ) is expressed as

$$Q_i = \sqrt{S_{iN}^2 - P_i^2} \quad (1)$$

The inverter is capable of supplying and drawing reactive power and it must match the load and grid requirements. Accordingly (2) and (3), assigns the reactive power limits for lagging and leading type of reactive demand, respectively.

$$Q_{i \max} = Q_i \quad (2)$$

$$Q_{i \max} = -Q_i \quad (3)$$

Hence, at a given instant, the total active power ( $P_T$ ), reactive power ( $Q_T$ ) and apparent power ( $S_T$ ) capabilities that the

inverters possess to match the reactive power demand of load and to supply the active power of PV systems to grid are represented by (4), (5) and (6), respectively.

$$P_T = \sum_{i=1}^m P_i \quad (4)$$

$$Q_T = \sum_{i=1}^m Q_i \quad (5)$$

$$S_T = \sqrt{P_T^2 + Q_T^2} \quad (6)$$

If output currents of all the inverters are equal, temperature of similar devices of the different inverters can be made equal. This can be realized if all the inverters operate with the same apparent power. Hence, the inverters are made to operate with the reference apparent power ( $S_{Tnew}$ ) to have uniform utilization and heating.

$$S_{Tnew} = S_T \div [(m+1) - i] \quad (7)$$

The algorithm evaluates the condition expressed by (8), and if  $S_{Tnew}$  exceeds  $S_{iN}$ , the reference apparent and reactive powers are set to values  $S_{iN}$  and  $Q_{imax}$  (or  $Q_{imin}$ ), respectively.

$$S_{Tnew} \leq S_{iN} \quad (8)$$

The algorithm then assigns the reference reactive power  $Q_{iref}$  and  $P_i$  for each inverter, where the active power references ( $P_i$ ) for the inverters are obtained from the MPPT. Once any inverter is assigned the reference active and reactive powers, the total unassigned active and reactive powers to be supplied by the remaining inverters are updated by subtracting the  $Q_{iref}$  and  $P_i$  assigned to the earlier inverters from  $P_T$  and  $Q_D$ , where  $Q_D$  is the reactive power demand of the load. The remaining active power ( $P_{Tn}$ ) to be supplied and reactive power demand to be met ( $Q_{Tn}$ ) is calculated as shown in (9), and (10), respectively.

$$P_{Tn} = P_T - \sum_{i=0}^{i-1} P_i \quad \text{where } P_0 = 0 \quad (9)$$

$$Q_{Tn} = Q_D - \sum_{i=0}^{i-1} Q_{iref} \quad \text{where } Q_{0ref} = 0 \quad (10)$$

Accordingly, the apparent power ( $S_i$ ) that  $i^{\text{th}}$  inverter must supply is obtained by (11)

$$S_i = \sqrt{P_{Tn}^2 + Q_{Tn}^2} / ((m+1) - i) \quad (11)$$

Hence, the reference reactive power for the  $i^{\text{th}}$  inverter is

$$Q_{iref} = \sqrt{S_i^2 - P_i^2} \quad (12)$$

### IV. SIMULATION RESULTS

To demonstrate the effectiveness of the above control strategy, microgrid system shown in Fig.1 is simulated in MATLAB/Simulink. In addition to the proposed control algorithm, two more control approaches: (optimal reactive power [15] and equal reactive power sharing [13]) are also evaluated and the results are compared with that obtained with the proposed control algorithm. Two different cases are considered for comparing the performance of this algorithm.

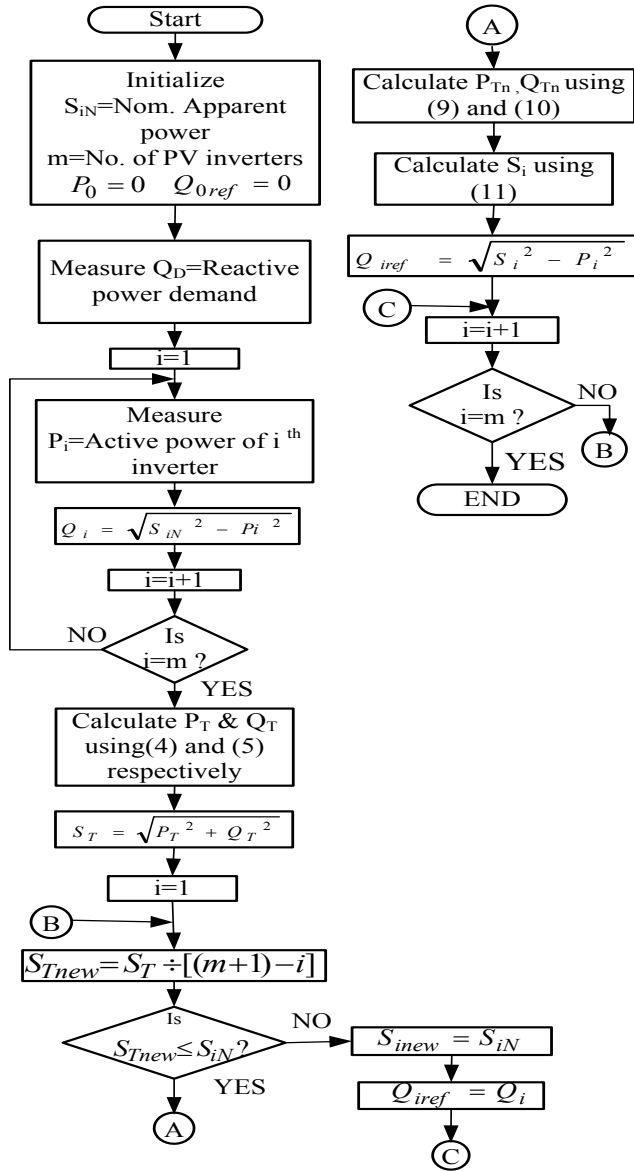


Fig. 4. Proposed reactive power sharing algorithm

In case (i), all the inverters are considered to have the equal ratings while in case (ii), inverters of unequal ratings are considered.

#### Case (i): Equal DG ratings

The parameters considered for evaluating the performance of the algorithms using the system of Fig. 1 are mentioned in TABLE I. As shown, all DGs are considered to have the equal nominal apparent power rating of 500 kVA.

TABLE I  
RATINGS AND PARAMETERS FOR THE SYSTEM OF FIG.1

Nominal power rating of DG1 ( $S_{1N}$ )	500 kVA
Nominal power rating of DG2 ( $S_{2N}$ )	500 kVA
Nominal power rating of DG3 ( $S_{3N}$ )	500 kVA
Nominal power rating of DG4 ( $S_{4N}$ )	500 kVA
Grid voltage( $V_g$ ), Frequency( $f$ )	415V, 50 Hz
Line parameter ( $Z_{01}=Z_{02}=Z_{03}=Z_{04}$ )	$L=100\mu\text{H}, R=2.07\text{m}\Omega, C_f=2500\mu\text{F}$
Load	1.92 MVA, 0.78 power factor (lag)
No of PV inverters ( $m$ )	4

Fig. 5 shows the results with the optimal reactive power sharing (ORPS) algorithm. Reactive power references for inverters shown in TABLE II are calculated using the ORPS algorithm of [15], while the active power references for the inverters are set at the value equal to the maximum power that the corresponding PV system generates at a given instant. The active power generated by PV arrays PV<sub>1</sub>, PV<sub>2</sub>, PV<sub>3</sub> and PV<sub>4</sub> till  $t=0.5\text{s}$  are 400kW, 300kW, 250kW and 450kW, respectively. A step change in irradiation on PV array PV<sub>1</sub> occurs at  $t=0.5\text{s}$ , which results in the output of PV<sub>1</sub> to decrease to 200kW. At  $t=1\text{s}$ , step change in irradiation on PV array PV<sub>3</sub> occurs, resulting into the change in the output power from 250kW to 400kW. Reactive power references for the inverters obtained with optimum reactive power control are mentioned in TABLE II. Fig. 5, shows active, reactive and apparent power of inverters 1 through 4.

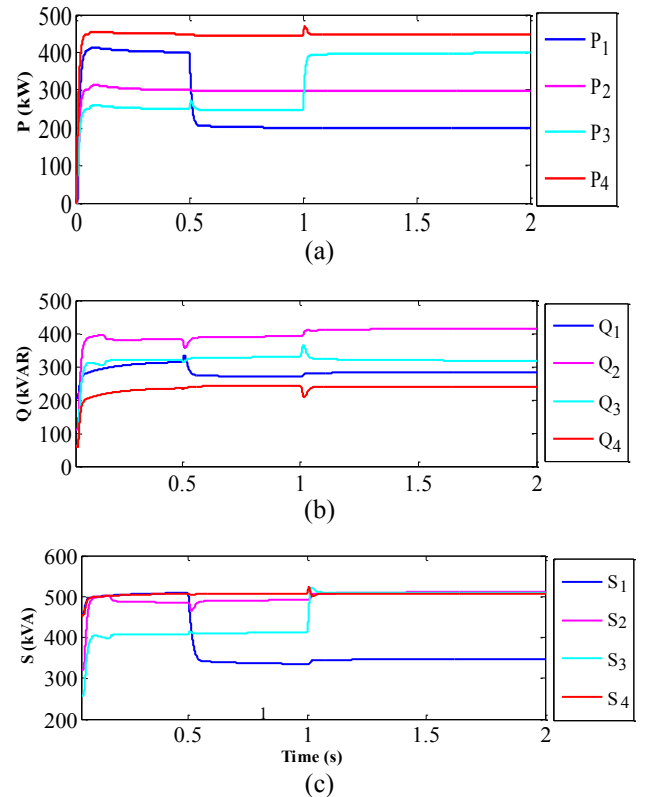


Fig. 5. Results with ORPS algorithm: (a) active power fed by DGs, (b) reactive power shared by the inverters, (c) apparent power of each inverter.

TABLE II  
UTILIZATION FACTOR OF EACH DG FOR ORPS ALGORITHM

Time Interval (s)	$P_i$ (kW)	$Q_{iref}$ (kVAR)	$S_i$ (kVA)	Util. Fac. $S_i/S_{Ni}$
$t=0-0.5$	400	300	500	1.00
	300	373	478	0.95
	250	310	398	0.79
	450	218	500	1.00
$t=0.5-1$	200	262	329	0.65
	300	392	493	0.98
	250	325	410	0.82
	450	218	500	1.00
$t=1-2$	200	282	345	0.69
	300	400	500	1.00
	400	300	500	1.00
	450	218	500	1.00

It is observed from Figs. 5(a) and (b) that, when  $P_1$  is decreased from 400kW to 200kW at  $t=0.5s$ ,  $Q_1$  changes from 300kVAR to 262kVAR. Not only  $Q_1$ , but  $Q_2$  through  $Q_4$  also changes. Similarly at  $t=1s$ , when  $P_3$  increases to 400kW,  $Q_1$  through  $Q_3$  changes. Thus, if power generated by any one of the PV array changes, the reactive power references and hence, the reactive power supplied by all the inverters change (except those which are operating at their limits  $S_{iN}$ ). Fig. 5(c) shows that inverters 1 and 4 operate at their maximum apparent power limits ( $S_{1N}$  and  $S_{4N}$ , respectively) till  $t=0.5s$ . At  $t=0.5s$ , when  $P_1$  reduces,  $Q_1$  also reduces simultaneously and hence, from  $t=0.5s$  to  $t=0.1s$  only inverter 4 operates at its full capacity. It is observed that the change in  $P_i$  and  $Q_i$  is such that the ratio  $P_i/Q_i$  remains equal for all the inverters that do not reach the rated capacity. An index defined as utilization factor ( $S_i/S_{iN}$ ) is used to indicate the extent to which the capacity of the inverter is utilized. It is also observed from the TABLE II that all the inverters are operating at different utilization factors. The utilization factors vary greatly showing that some of the inverters operate much below their rated capacity when some others have already hit their limits. For example, inverter-1 operates with the lowest utilization factor (0.65 from  $t=0.5s$  till 1s and 0.69 from  $t=1s$  till 2s) while inverter-4 is operating at its limit. The unequal utilization of the inverters, not only results into unequal losses, efficiency and heating of different inverters, but may damage the inverters that continuously operate at their apparent power limits.

Fig. 6 shows the results obtained with equal reactive power sharing (ERPS) algorithm [13], according to which reactive power demand is equally shared amongst the inverters. The

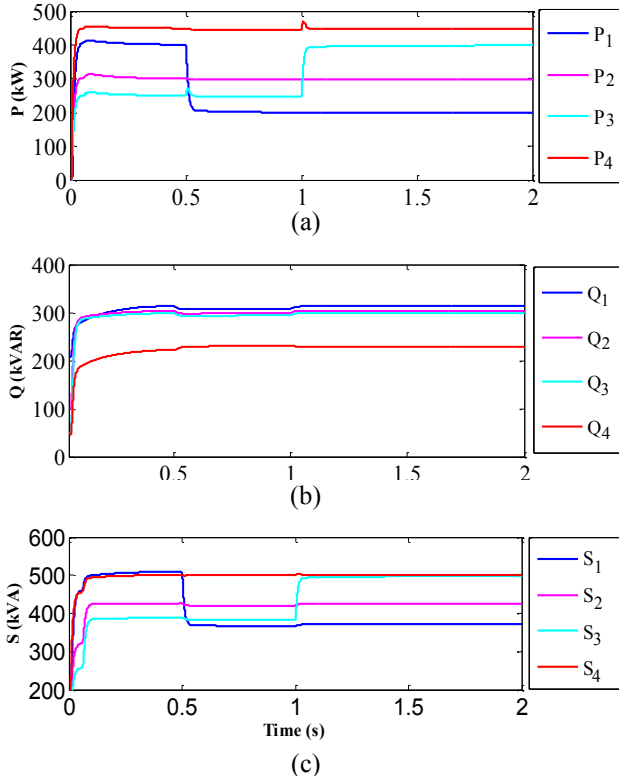


Fig. 6. Results with ERPS algorithm: (a) active power fed by DGs, (b) reactive power shared by the inverters, (c) apparent power of each inverter

irradiation pattern on the PV array is considered the same as that considered for the evaluation of ORPS approach. Fig. 6

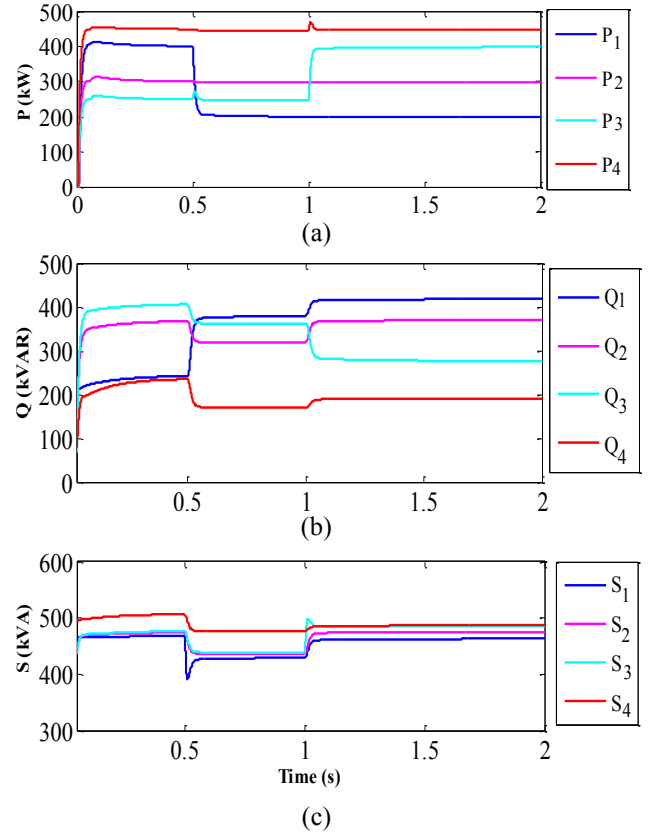


Fig. 7. Results with Proposed algorithm: (a) active power fed by DGs, (b) reactive power shared by the inverters, (c) apparent power of each inverter shows active, reactive and apparent powers respectively, of inverters 1 through 4.

If it is intended to meet the total reactive power demand of the load mentioned in TABLE I (1200kVAR) through the inverters 1 through 4 using ERPS control, each inverter must output 300kVAR. Hence, the reference reactive power for inverter 1,2 and 3 are set equal to 300kVAR (reactive power demand of load = 1200kVAR) while for inverter- 4 which hits its apparent power limit, it is restricted to 218 kVAR. It is observed from Figs. 6(a)-(c), and TABLE III that, even if the active power supplied by the PV array changes, the effect is not observed in the reactive power sharing. It is also evident from Fig. 6(c) that inverter-4 continuously operates at its rated capacity of 500kVA. Inverters 1 and 3 also operate at their rated capacities for some time. It is also observed that  $S_i$  (for  $i=1, 2$  and 4) remains almost constant for  $t=0.5s$  to 2s inspite of the change in  $P_3$  at  $t=1s$ . The reason being no change in  $P_i$  and  $Q_i$  (for  $i=1, 2$  and 4) for this period. Unlike ORPS the reactive power demand of the load is not met fully inspite of the fact that many inverters still operate below their rated limits. Thus, the inverters are not utilized optimally and also the percentage utilization of all the inverters varies greatly.

Fig.7 shows performance with proposed algorithm when same pattern of irradiation on the PV array as that considered for ORPS and ERPS is maintained. At  $t=0.5s$ , when the irradiation of  $PV_1$  decreases resulting into the decrease in the

TABLE III  
UTILIZATION FACTOR OF EACH DG FOR ERPS ALGORITHM

Time Interval(s)	$P_i$ (kW)	$Q_{iref}$ (kVAR)	$S_i$ (kVA)	Uti. Fac. $S_i/S_{Ni}$
t=0-0.5	400	300	500	1.00
	300	300	424	0.84
	250	300	390	0.78
	450	218	500	1.00
t=0.5-1	200	300	360	0.72
	300	300	424	0.84
	250	300	390	0.78
	450	218	500	1.00
t=1-2	200	300	360	0.72
	300	300	424	0.84
	400	300	500	1.00
	450	218	500	1.00

output power of inverter 1, the reactive power of inverter 1 increases. Simultaneously, the reactive powers of all other inverters decrease in spite of the fact that there is no change in the power output from PV arrays PV<sub>2</sub>, PV<sub>3</sub> and PV<sub>4</sub>. This results into minimizing the gap of percentage utilization of different inverters. Similarly, at t=1s when P<sub>3</sub> changes from 250kW to 400kW, reactive power of all the inverters changes to achieve better sharing of the active and reactive power amongst them. TABLE IV shows the active, reactive and apparent powers shared by the inverters over the different periods. Unlike ORPS and ERPS, the utilization factors vary little for all the DGs indicating uniform loading of the inverters.

The three algorithms are tested even with a different load having a leading power factor (PF). TABLE V shows the results obtained with a load of 1.16 MVA, 0.86 power factor (lead). It is observed that even with leading power factor, proposed algorithm performance is superior. Standard deviations of the

TABLE IV  
UTILIZATION FACTOR OF EACH DG FOR PROPOSED ALGORITHM

Time Interval(s)	$P_i$ (kW)	$Q_{iref}$ (kVAR)	$S_i$ (kVA)	Uti. Fac. $S_i/S_{Ni}$
t=0-0.5	400	229	460	0.92
	300	354	464	0.92
	250	393	466	0.93
	450	222	500	1.00
t=0.5-1	200	374	424	0.85
	300	311	432	0.86
	250	355	434	0.86
	450	159	477	0.95
t=1-2	200	405	452	0.90
	300	356	465	0.93
	400	262	478	0.95
	450	175	482	0.96

TABLE V  
COMPARISON OF THE VARIOUS ALGORITHM FOR LEADING PF LOAD

Algorithms	$P_i$ (kW)	$Q_{iref}$ (kVAR)	$S_i$ (kVA)	Uti. Fac. $S_i/S_{Ni}$
ORPS	300	-180	350	0.70
	200	-120	233	0.46
	150	-90	175	0.35
	350	-210	408	0.82
ERPS	300	-150	335	0.67
	200	-150	250	0.50
	150	-150	212	0.42
	350	-150	380	0.76
Proposed	300	0	300	0.60
	200	-233	307	0.61
	150	-271	309	0.61
	350	-96	362	0.72

utilization factors of the various inverters are calculated, to quantify the effectiveness of the algorithm to distribute the apparent power equally amongst the inverters. Standard deviations of the utilization factors for the three schemes for the case represented by TABLE V are 0.204, 0.147 and 0.055. The least the standard deviation better is the performance.

#### Case (ii): Unequal DG ratings

The three algorithms are also evaluated for the case when all DGs of the system shown in Fig. 1 have unequal ratings. The nominal ratings for the DGs are mentioned in TABLE VI. The load, line parameters, capacitance C and the grid voltage are considered same as that of case (i).

In this case the active power generated by PV arrays PV<sub>1</sub>, PV<sub>2</sub>, PV<sub>3</sub> and PV<sub>4</sub> are 200kW, 300kW, 400kW and 500kW, respectively. A step increase in irradiation on PV array PV<sub>1</sub> occurs at t=0.5s, which results in the output of PV<sub>1</sub> to increase to 300kW. At t=1s, irradiation on PV array PV<sub>3</sub> decreases suddenly, resulting into the change in its output power from 400kW to 200kW. The active, reactive and apparent power sharing by inverters 1 through 4 with ORPS control are displayed in Fig. 8 and the results are quantified in TABLE VII.

Figs. 8(a) and (b) shows that when PV<sub>1</sub> is increased from 200kW to 300kW at t=0.5s, Q<sub>1</sub> also increases from 171kVAR to 240kVAR. Hence its apparent power increases, leading to its utilization factor of 0.96. The reactive powers of inverters 2 through 4 decrease with their active powers still at the same values. Thus, S<sub>2</sub> through S<sub>4</sub> decrease lowering the utilization of inverters 2 through 4. This increases the miss-match in the utilization factors. The miss-match further increases after t=1s, when the output power of PV<sub>3</sub> decreases from 400kW to 200kW. The decrease in P<sub>3</sub> at t=1s is associated with the simultaneous decrease in Q<sub>3</sub>. Hence, to meet the reactive power demand of the load, more reactive power needs to be supplied by inverters 1, 2 and 4. Hence, while the utilization factor of inverter-3 decreases, utilization factor of other inverter increases. Thus, inverter-3 is the least utilized inverter with utilization factor of 0.45 while inverter-1 is fully utilized with the utilization factor of 1.00. Fig. 5(c) also highlights that after t=1s, inverter-1 operates at its apparent power limit (S<sub>IN</sub>). It is observed from TABLE VII that the percentage change (decrease) in utilization factor of inverter-3 in response to the decrease in output power P<sub>3</sub> of inverter-3 is -47%.

Fig. 9 shows the power shared by DGs (having ratings mentioned in TABLE VI) when operated with ERPS algorithm. The same shading pattern, adopted earlier for ORPS of case (ii), is considered. The reference reactive power for all the inverters is set equal to 300kVAR to meet the load's reactive power demand (TABLE VIII). Fig. 9(c) shows that after t=0.5s, inverter-1 continuously operates at its rated capacity 400kVA and hence, is unable to meet its desired reactive power share of 300kVAR. Like earlier case with ERPS control, the reactive

TABLE VI  
Ratings Of Dg Of The System Of Fig.1 For Case (ii)

Nominal power rating of DG1 (S <sub>1N</sub> )	400 kVA
Nominal power rating of DG2 (S <sub>2N</sub> )	500 kVA
Nominal power rating of DG3 (S <sub>3N</sub> )	600 kVA
Nominal power rating of DG4 (S <sub>4N</sub> )	700 kVA

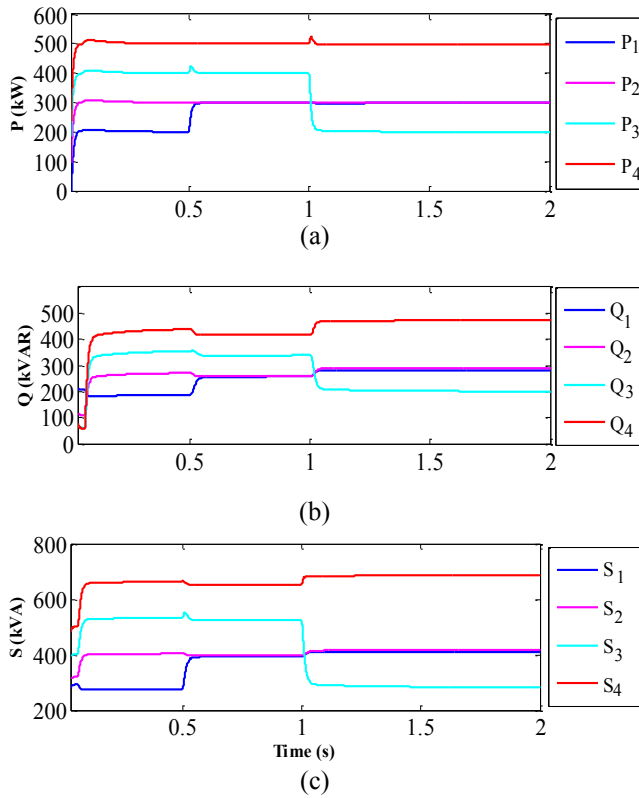


Fig. 8. Results with ORPS algorithm: (a) active power fed by DGs, (b) reactive power shared by the inverters, (c) apparent power of each inverter

power demand of the load is once again not met fully. Thus, the inverters are not utilized optimally. Significant variation in utilization factors is observed. Also the percentage change in the utilization factor of inverter-3 due to change in  $P_3$  at  $t=1$ s is  $-27.7\%$ . The power sharing, the utilization factors and the variation in the utilization factors are highly dependent on the nominal ratings of the inverters and the load.

Fig. 10 shows performance of proposed algorithm with same pattern of irradiation on the PV array as considered earlier for ERPS and ORPS algorithm of case (ii). It is observed from TABLE IX that during  $t=0$ s to  $t=0.5$ s, the proposed algorithm tries to share the apparent power equally amongst all the inverters. Hence, as the inverter-1 reaches its limit, it is operated at 400kVA (100% capacity), while inverters 2, 3 and 4 are operated around 500kVA demonstrating the tendency of equalizing the reactive power sharing. At  $t=0.5$ s, when the irradiation of  $PV_1$  increases resulting into the increase in the

TABLE VII  
UTILIZATION FACTOR OF EACH DG FOR ORPS ALGORITHM

Time Interval(s)	$P_i$ (kW)	$Q_{ref}$ (kVAR)	$S_i$ (kVA)	Uti. Fac. $S_i/S_{Ni}$
t=0-0.5	200	171	263	0.65
	300	257	395	0.79
	400	342	526	0.87
	500	425	656	0.93
t=0.5-1	300	240	384	0.96
	300	240	384	0.76
	400	320	512	0.85
	500	400	640	0.91
t=1-2	300	276	407	1.00
	300	277	408	0.81
	200	185	272	0.45
	500	462	680	0.97

output power of inverter 1, the output reactive power of inverter 1 decreases. Simultaneously the reactive powers of all other inverters increase.

TABLE VIII  
UTILIZATION FACTOR OF EACH DG FOR ERPS ALGORITHM

Time Interval(s)	$P_i$ (kW)	$Q_{ref}$ (kVAR)	$S_i$ (kVA)	Uti. Fac. $S_i/S_{Ni}$
t=0-0.5	200	300	360	0.90
	300	300	424	0.84
	400	300	500	0.83
	500	300	583	0.83
t=0.5-1	300	265	400	1.00
	300	300	424	0.84
	400	300	500	0.83
	500	300	547	0.78
t=1-2	200	265	400	1.00
	300	300	424	0.84
	200	300	360	0.60
	500	300	547	0.78

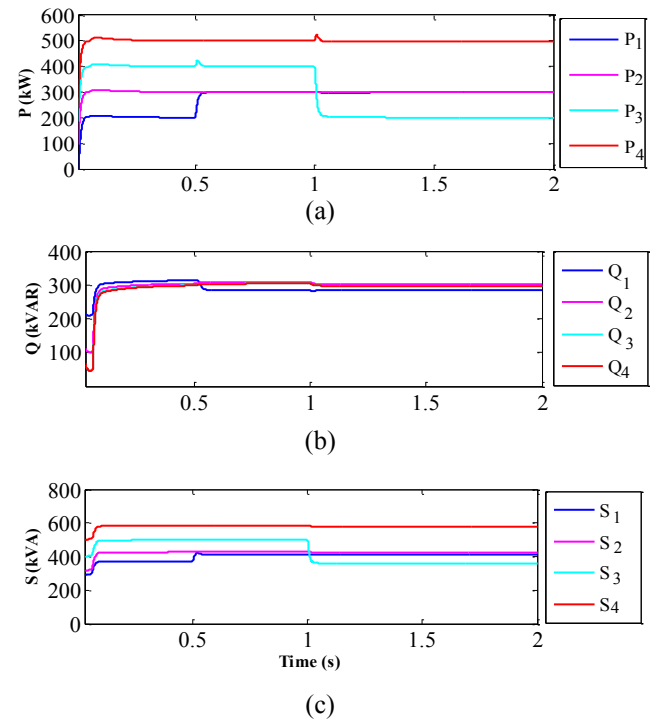


Fig. 9. Results with ERPS algorithm (a) active power fed by DGs, (b) reactive power shared by the inverters, (c) apparent power of each inverter

This results into minimizing the miss-match in the reactive

powers of the inverters and hence, reduces the gap of percentage utilization of different inverters. Thus, the algorithm inherently has the feature of minimizing the mismatch. But still the mismatch is relatively large. This is due to the equal apparent power sharing principle of the algorithm, which inspite of the unequal nominal kVA rating of the inverters, tries to allocate the apparent power equally amongst the DG inverters. Hence, it results into the unequal utilization factor of the DGs. At  $t=1$ s when  $P_3$  changes from 400 kW to 200kW,  $Q_3$  increases and  $Q_4$  and  $Q_2$  decrease to achieve better power sharing amongst the inverters. The least utilization factor of 0.6 is observed for inverter-3. It is observed from TABLE IX that percentage decrease in utilization factor for inverter-3 (due to

change in  $P_3$  at  $t=1s$  is -13.8%, which is relatively smaller than that observed with ORPS (-47%) and ERPS (-27.7%).

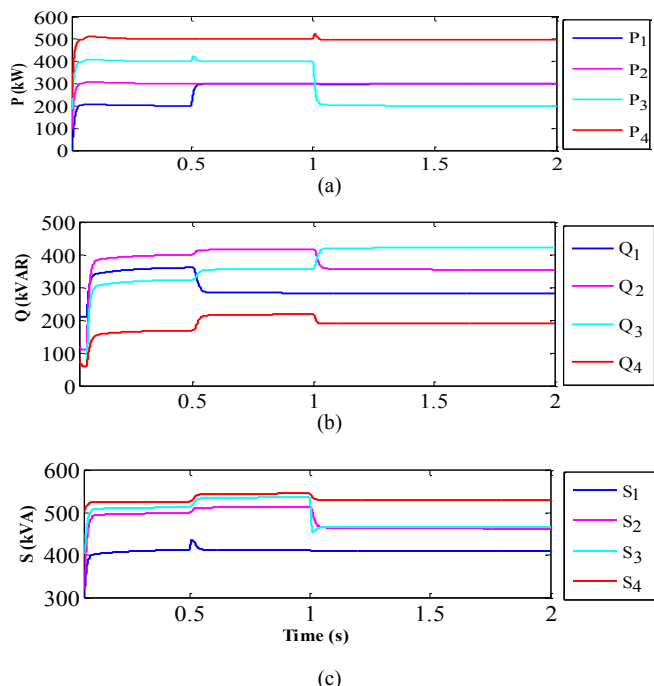


Fig.10. Results with proposed algorithm (a)active power fed by DGs, (b) reactive power shared by the inverters, (c)apparent power of each inverter

TABLE IX  
UTILIZATION FACTOR OF EACH DG FOR PROPOSED ALGORITHM

Time Interval(s)	$P_i$ (kW)	$Q_{ref}$ (kVAR)	$S_i$ (kVA)	Uti. Fac. $S_i/S_{Ni}$
$t=0-0.5$	200	346	399	0.99
	300	388	500	0.98
	400	310	500	0.83
	500	154	520	0.74
$t=0.5-1$	300	265	399	0.99
	300	400	500	0.99
	400	338	523	0.87
	500	197	537	0.76
$t=1-2$	300	265	399	0.99
	300	344	450	0.90
	200	412	450	0.75
	500	179	500	0.75

## V. CONCLUSION

In case of renewable energy source (PV or wind) based DG, the reactive power that it can supply varies as the active power supplied by it changes. The conventional algorithm, which relies on the sharing of equal reactive power amongst the inverters, fails under such case. Not only the inverter gets overloaded but also the distribution of the total apparent power amongst the inverters vary greatly leading to uneven percentage utilization of the inverters. The optimal reactive algorithm also suffers from similar drawbacks. It is observed that the proposed algorithm maintains operation of all inverters within their nominal ratings and yet they are able to match the total reactive power demand of the load. As the reactive power assigned to the inverters is linked with the available reactive power capabilities, the inverter that supplies lesser active power is controlled to share a greater amount of reactive power. If the DG inverters have equal kVA ratings, then with the proposed

algorithm, not only the apparent power sharing is better than other algorithms but the utilization factors of the inverters are also nearly similar. However, as the algorithm tries to share the apparent power equally amongst the inverters, the utilization factors are not the same for the inverters of unequal kVA ratings. But the algorithm always operates to minimize the miss-match in the utilization factors. Hence, with the proposed approach, comparatively better apparent power sharing is observed leading to reduction in the variation of percentage utilization of the inverters.

## REFERENCES

- [1] Y. Huang, F. Z. Peng, J. Wang and D. Yoo "Survey of power conditioning system for PV power generation," *Power Electronics Specialist Conference, PESC 2006*, pp.1-6, June 2006.
- [2] Y. Riffonneau, S. Bacha, F. Barruel, and S. Ploix "Optimal power flow management for grid connected PV systems with batteries" *IEEE Trans. Sustainable energy*, vol. 2, no. 3, pp.309-320 July 2011.
- [3] R. H. Lasseter and P. Paigi, "Microgrid: A conceptual solution," presented at the *IEEE Power Electron. Spec. Conf. Aachen*, Germany, 2004.
- [4] N. Eghtedarpour and E. Farjah, "Power control and management in a hybrid AC/DC microgrid," *IEEE Trans. Smart Grid*, vol. 5, no. 3, pp. 1494–1505, May 2014.
- [5] C.T. Lee, C.C. Chu, and P.T. Cheng, "A new droop control method for the autonomous operation of distributed energy resource s interface converters," *IEEE Trans. Power Electron.*, vol. 28, no. 4, pp. 1980–1993, April 2013.
- [6] Q. Zhong, "Robust Droop Controller for Accurate Proportional Load Sharing Among Inverters Operated in Parallel," *IEEE Trans. Ind. Electronics*, vol. 60, no. 4, pp. 3747-3459, April 2013.
- [7] I. U. Nutkani, P. C. Loh, and F. Blaabjerg, "Droop scheme with considering of operating cost," *IEEE Trans. Power Electron.*, vol. 29, no. 3, pp. 1047–1052, March 2014.
- [8] A. Bidram and A. Davoudi, "Hierarchical structure of microgrids control system," *IEEE Trans. Smart Grid*, vol. 3, no. 4, pp. 1963–1976, December 2012.
- [9] J. He, and Y. Li" An accurate reactive power sharing control strategy for DG units in a microgrid" 8th International Conference on Power Electronics - ECCE Asia, the Shilla Jeju, Korea. May 30-June 3, 2011.
- [10] A. Milczarek, M. Malinowski and J. M. Guerrero" Reactive power management in islanded microgrid—proportional power sharing in hierarchical droop control" *IEEE Trans. Smart grid*, vol. 6, no. 4, pp. 1631-1638, July 2015.
- [11] K. Turitsyn, Petrusulc, S. Backhaus, and M. Chertkov " Options for control of reactive power by distributed photovoltaic generators" *Proceedings of the IEEE*, vol. 99, No. 6, pp 1063-1073, June 2011.
- [12] F. Olivier, P. Aristidou, D. Ernst, and T. V. Cutsem, "Active management of low-voltage networks for mitigating over voltages due to photovoltaic units" *IEEE Trans. Smart grid*, vol. 7, NO. 2, pp. 926-93, March 2016.
- [13] A. Micallef, M. Apap, J. M. Guerrero, and J. C. Vasquez, " Reactive power sharing and voltage harmonic distortion compensation of droop controlled single phase islanded microgrids" *IEEE Trans. Smart grid*, vol. 5, no. 3, pp. 1149-1158, May 2014.
- [14] S. Duan, Y. Meng, J. Xiong, Y. Kang and J. Chen. "Parallel operation technique of voltage source inverters in UPS," *IEEE International Conference on Power Electronics and Drive Systems*, Hong Kong, 883 –887, PEDS'99.
- [15] Z.Wang. K.M., Passino, J.Wang, "Optimal reactive power allocation in large scale grid connected photovoltaic system", *Journal of optimization theory and application*, November 2015.
- [16] A. Micallef, M. Apap and C. SpiteriStaines, J. M. Guerrero Zapata" Secondary control for reactive power sharing and voltage amplitude restoration in droop-controlled islanded microGrids " 3<sup>rd</sup> IEEE International Symposium on Power Electronics for Distributed Generation Systems (PEDG) 2012.

- [17] T. L. Vandoorn, B. Renders, L. Degroote, B. Meersman, and L. Vandeveldel, "Controllable harmonic current sharing in islanded microgrids: DG units with programmable resistive behavior toward harmonics," *IEEE Trans. Power Del.*, vol. 27, no. 3, pp. 1405–1414, July 2012.
- [18] Adhikari and Fangxing Li, "Coordinated V-f and P-Q control of solar photovoltaic generators with MPPT and battery storage in microgrids" *IEEE trans. on smart grid*, vol. 5, no. 3, pp 1270-1281, May 2014.
- [19] H. Mahmood, D. Michaelson, and J. Jiang, "Accurate reactive power sharing in an islanded microgrid using adaptive virtual impedances" *IEEE Tran. Power electron.* vol. 30, no. 3, pp. 1605-1617, March 2015.
- [20] J. W. Smith, W. Sunderman, R. Dugan, Brian Seal, "Smart inverter Volt/Var control functions for high penetration of PV on distribution Systems "Power system conference and Exposition (PACE) 2011..



**Urvi Patel** received B.E degree in electrical engineering from the S.V. Regional College of Engineering and Technology (now S.V. National Institute of Technology), South Gujarat University, Surat, India, in 2000, and the M.E. degree in Electrical engineering in 2009 from the M. S. University, Baroda, India

She is currently working as an Assistant Professor in the Department of Electrical Engineering at C. K. Pithawalla College of Engineering and Technology, Surat and pursuing Ph.D. in electrical engineering. Her current research interests include distributed generation, renewable energy and microgrid issues. She is a Life Member of the Indian Society for Technical Education and a member of IEEE.



**Hiren Patel** received the B.E. degree in electrical engineering from the S.V. Regional College of Engineering and Technology (now S.V. National Institute of Technology), South Gujarat University, Surat, India, in 1996, and M. Tech. in energy systems and PhD in Electrical Engineering degree

from the Indian Institute of Technology Bombay (IITB), Mumbai, India in 2003 and 2009, respectively. He is working as a Professor and Dean, R&D at the Sarvajanic College of Engineering and Technology, Surat.

His current research interests include computer aided simulation techniques, distributed generation, and renewable energy, especially energy extraction from photovoltaic arrays. He has to his name several publications in international and national journals and conferences. He is a Life Member of the Indian Society for Technical Education and the Institute of Engineers.